3. DISCUSSION AND CONCLUSIONS

The radiation performance of a single feed circularly polarized stacked arrangement of edge truncated elliptical and conventional circular patches is presented in this communication and results are compared with that of a single layered edge truncated elliptical patch antenna. Though the single feed single layer edge truncated elliptical patch antenna presents circular polarization but its axial ratio bandwidth, impedance bandwidth and gain are low. Therefore this geometry is modified in this communication and a two layered stacked arrangement is proposed with much improved performance. By considering present arrangement, both impedance bandwidth and gain of antenna are improved to a great extent. Circular polarization with improved axial ratio bandwidth is achieved with present arrangement. The reported impedance bandwidth and axial ratio bandwidth are 27.9 and 3.33%, respectively which are significantly higher than that of conventional or edge truncated elliptical patch antenna geometry. The obtained results suggest that proposed antenna with little more improvement may become very useful for modern communication systems.

REFERENCES

1. R. Garg, P. Bhartia, I. Bahl, and A. Ittipiboon, Microstrip antenna design handbook, Artech House, Norwood, 2001.
2. K.L. Wong, Compact and broadband microstrip antennas, Wiley, New York, 2003.
3. L.C. Shen, The elliptical microstrip antenna with circular polarization, IEEE Trans Antennas Propag 29 (1981), 90–94.
4. N. Hercovici, Z. Sipus and D. Bonefacic, Circularly polarized single-fed wide band microstrip patch, IEEE Trans Antennas Propag 51 (2003), 1277–1280.
5. S. Egashira and E. Nishiyama, Stacked microstrip antennas with wide bandwidth and high gain, IEEE Trans Antennas Propag 44 (1996), 1533–1534.
6. J.G. Kretzschmar, Wave propagation in hollow conducting elliptical waveguides, IEEE Trans Microwave Theory Tech 18 (1970), 547–554.
7. Zealand Software, Inc. Zeland Software, IE3D Software, Release 8, Zealand Software, Inc., Freemont.

PLANAR STRIP MONOPOLE WITH A CHIP-CAPACITOR-LOADED LOOP RADIATING FEED FOR LTE/WWAN SLIM MOBILE PHONE APPLICATION

Shu-Chuan Chen and Kin-Lu Wong
Department of Electrical Engineering, National Sun Yat-sen University, Kaohsiung 80424, Taiwan; Corresponding author: chensc@ema.ee.nsysu.edu.tw

ABSTRACT: *A small-size wideband internal mobile phone antenna formed by a planar strip monopole with a chip-capacitor-loaded loop radiating feed for achieving eight-band long term evolution/wireless wide area network operation in the 698–960 and 1710–2690 MHz bands is presented. The antenna is suitable to be disposed on a small no-ground board space (15×45 mm^2) of the system circuit board and enclosed by an L-shaped system ground plane of the mobile phone. On the protruded ground of the L-shaped system ground plane, a universal series bus connector for the data port of the mobile phone can be accommodated without affecting the antenna performances. The antenna also shows a low profile of 3 mm above the circuit board, which makes it very promising for slim mobile phone applications. The proposed antenna was fabricated and tested. Measured and simulated results are presented. The specific absorption rate results of the antenna are also analyzed.* © 2011 Wiley Periodicals, Inc. Microwave Opt Technol Lett 53:952–958, 2011; View this article online at wileyonlinelibrary.com. DOI 10.1002/mop.25845

1. INTRODUCTION

Owing to the recent introduction of the long term evolution (LTE) operation [1] for mobile broadband services, the mobile devices such as the notebook computers and mobile phones in the near future are expected to be capable of both the LTE and wireless wide area network (WWAN) operations. For this application, the internal antenna in the mobile device should provide two wide operating bands of at least 698–960 and 1710–2690 MHz to cover three LTE bands (LTE700/2300/2500 in the 698–787/2300–2400/2500–2690 MHz bands) and five WWAN bands (GSM850/900/1800/1900/UMTS in the 824–894/880–960/1710–1880/1850–1990/1920–2170 MHz bands). Several promising eight-band LTE/ WWAN internal antennas have also been recently reported [2–6]. For the mobile phone applications, however, these reported LTE/WWAN antennas are generally employed at the entire edge of the system circuit board of the mobile phone [3–6]. This limits the flexibility of the antenna's integration inside the mobile phone.

In this article, we present a simple internal antenna design for eight-band LTE/WWAN operation in the mobile phone, especially in the slim mobile phone which usually requires the thickness of the embedded antenna to be less than 4 mm [7–13]. The proposed antenna has a low profile of 3 mm only and is suitable to be disposed on a small no-ground board space of 15 × 45 mm^2 at either the top or bottom edge of the system circuit board. Further, the no-ground board space occupies only a fractional portion of the edge and is enclosed by an L-shaped system ground plane of the mobile phone. A universal series bus (USB) connector [14] for the data port of the mobile phone can be disposed on the protruded ground of the L-shaped system ground plane. Note that other than the USB connector, the associated electronic elements such as an embedded digital camera [15, 16] or a loudspeaker [17–19] can also be disposed on the protruded ground. The proposed structure can improve the integration flexibility of the internal LTE/WWAN antenna inside the mobile phone.

In addition, a new technique of using a chip-capacitor-loaded loop radiating feed to generate an additional resonant mode for widening the antenna's upper-band bandwidth and also lead to a dual-resonance excitation of the antenna's lower band is applied in this study. With the applied technique, a planar strip monopole can provide two wide operating bands, with the lower one covering the LTE700/GSM850/900 operation (698–960 MHz) and the upper one covering the GSM1800/1900/UMTS/LTE2300/2500 operation (1710–2690 MHz). Details of the operating principle of the proposed antenna are discussed. Results of
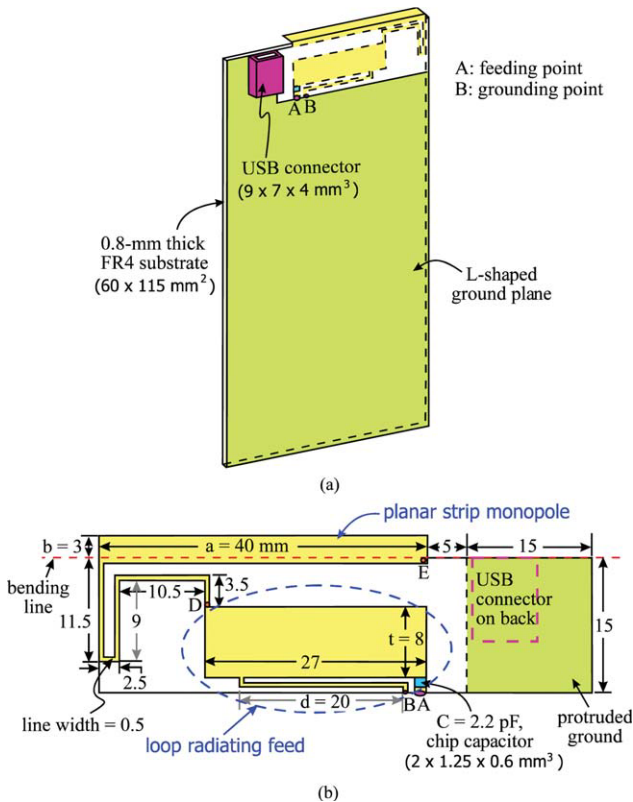
Figure 1 (a) Geometry of the planar strip monopole with a chip-capacitor-loaded loop radiating feed for LTE/WWAN operation in the slim mobile phone. (b) Dimensions of the metal pattern of the antenna. [Color figure can be viewed in the online issue, which is available at wileyonlinelibrary.com]

the proposed antenna including its specific absorption rate (SAR) [20, 21] values are also presented.

2. PROPOSED ANTENNA

Figure 1(a) shows the geometry of the proposed antenna, and dimensions of the metal pattern of the antenna are given in Figure 1(b). The antenna is a planar strip monopole connected with a chip-capacitor-loaded loop radiating feed. The chip capacitor has a size of $2 \times 1.25 \times 0.6$ mm^3 and is selected to have a capacitance C of 2.2 pF, which can provide a similar function as the coupling feed used for the reported internal WWAN antennas in [22–25] to generate a dual-resonance excitation for the antenna's lower band. In the proposed design, this loaded chip capacitor makes the resonant mode contributed by the planar strip monopole become a dual-resonant mode such that a wide lower band of bandwidth about 300 MHz is achieved for the proposed antenna.

The loop radiating feed alone also contributes an additional resonant mode at about 1800 MHz, which combines with a higher-order resonant mode contributed by the planar strip monopole at about 2700 MHz to form a wide upper band of bandwidth larger than 1 GHz for the proposed antenna. The wide lower and upper bands allow the antenna to cover the eight-band LTE/WWAN operation in the 698–960 and 1710–2690 MHz bands.

Note that the performances of the loop radiating feed can be controlled by adjusting the width t of its widened section and the position d of its grounding point B. Varying the position d leads to the length variations of the loop radiating feed from point A (the feeding point) to point B, such that the excited resonant mode contributed by the loop radiating feed can be shifted to lower or higher frequencies. Increasing the width t of the widened section can lead to smooth excited surface current distributions on the loop radiating feed, which can result in impedance matching improvement for all the three resonant modes of the antenna (one at about 1800 MHz contributed by the loop radiating feed and two at about 850 and 2700 MHz by the planar strip monopole).

In the planar strip monopole, the end section is widened and bent to decrease its occupying board space in the system circuit board of the mobile phone, which uses a 0.8-mm thick FR4 substrate of relative permittivity 4.4 and size 60×115 mm^2. Similar to the parameters t and d of the loop radiating feed, varying the width b of the bent section mainly improves the impedance matching of the excited resonant modes contributed by the planar strip monopole, while varying the length a of the bent section can control the frequency shifting of the excited resonant modes contributed by the planar strip monopole.

Further, the proposed antenna is disposed on the no-ground portion of 15×45 mm^2 shown in the figure. The antenna is also enclosed by an L-shaped system ground plane printed on the back side of the system circuit board. A USB connector is mounted on the protruded ground of the L-shaped system ground plane in the study. Although a USB connector is nearby the antenna, no noticeable effects on the performances of the proposed antenna are seen.

3. RESULTS AND DISCUSSION

The proposed antenna was fabricated and tested. Figure 2 shows the photos of the front and back views of the fabricated antenna. Note that for testing the antenna in the experiment, a 50-Ω microstrip feedline is printed on the system circuit board as seen in the photo. One end of the feedline is connected to point A, the feeding point of the antenna, while the other end (point A′)
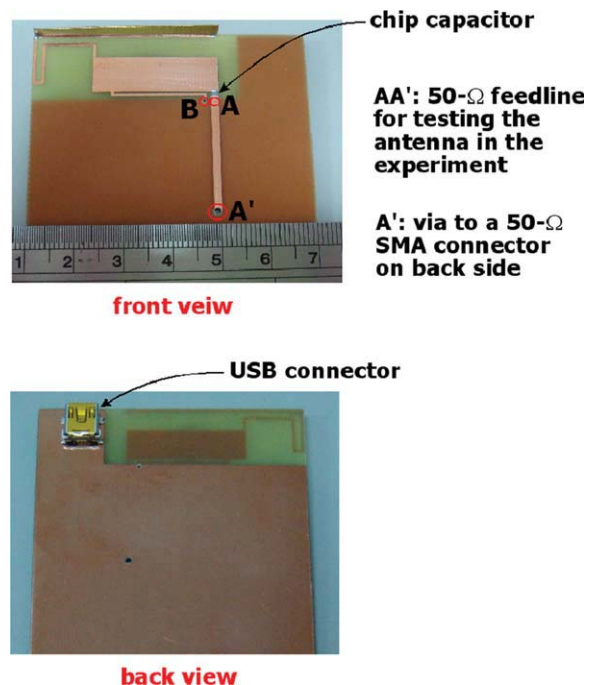
Figure 2 Photos of the front and back views of the fabricated antenna. [Color figure can be viewed in the online issue, which is available at wileyonlinelibrary.com]
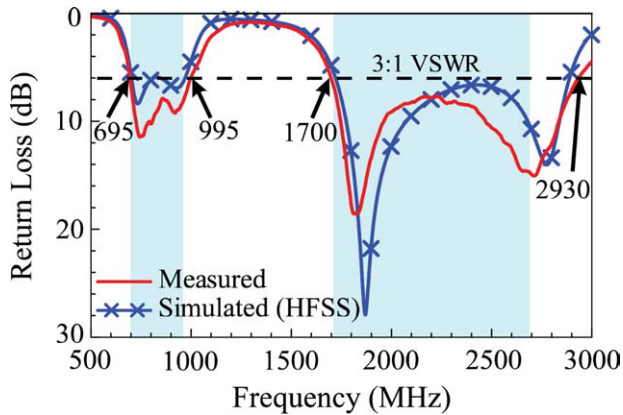
Figure 3 Measured and simulated return loss of the fabricated antenna. [Color figure can be viewed in the online issue, which is available at wileyonlinelibrary.com]

is connected to a 50-Ω SMA connector (not shown in the photo) on the back side of the circuit board through a via-hole. Results of the measured and simulated return loss for the fabricated antenna are presented in Figure 3. The simulated results are obtained using Ansoft simulation software high frequency structure simulator (HFSS) [26], and agreement between the simulation and measurement is seen from the results. Two wide operating bands are obtained for the proposed antenna. Based on the 3:1 VSWR bandwidth definition, which is widely used as the design specification of the internal WWAN mobile phone antenna, the measured bandwidth of the lower and upper bands respectively cover the desired LTE700/GSM850/900 and GSM1800/1900/UMTS/LTE2300/2500 operations.
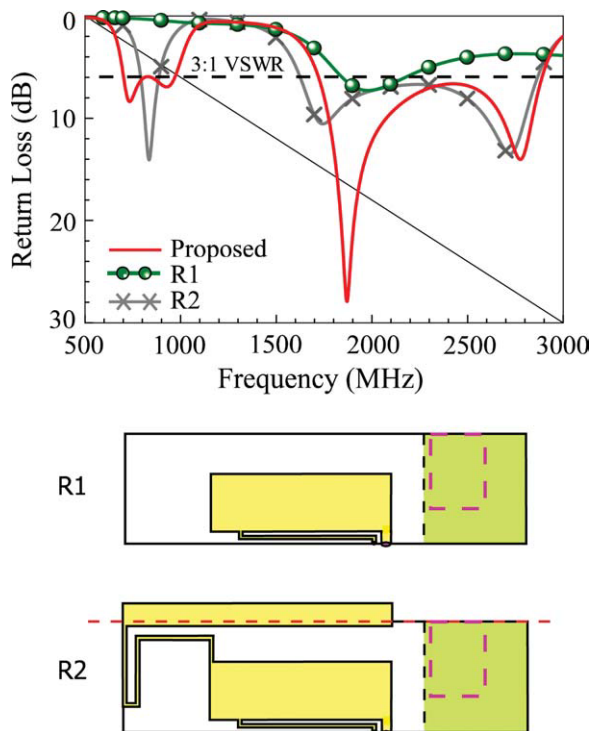
Figure 4 Simulated return loss for the proposed antenna, the loop radiating feed only (R1), and the strip monopole with the loop radiating feed only (R2). [Color figure can be viewed in the online issue, which is available at wileyonlinelibrary.com]

To analyze the operating principle of the proposed antenna, Figure 4 shows the simulated return loss for the proposed antenna, the loop radiating feed only (R1), and the strip monopole with the loop radiating feed only (R2). For R1, there is one resonant mode excited in the desired upper band. This resonant mode is contributed by the loop radiating feed. When the planar strip monopole is added to the loop radiation feed, two additional resonant modes are generated, with the lower one at about 850 MHz and the higher one at about 2700 MHz. By further loading a chip capacitor of 2.2 pF near the feeding point A, the resonant mode at about 850 MHz contributed by the planar strip monopole becomes a dual-resonance mode, which forms a wide operating band for the antenna's lower band. Effects of the loaded chip capacitor are hence similar to that of using a coupling feed in the reported internal WWAN antennas in [22–25] to generate a dual-resonance excitation for the antenna's lower band. On the other hand, the other two resonant modes contributed respectively by the planar strip monopole and the loop radiating feed are formed into a wide operating band for the antenna's upper band.

Figure 5 shows the simulated return loss for the proposed antenna as a function of the length a and width b of the bent end-section of the strip monopole. Other dimensions are the same as given in Figure 1. Results for the length a varied from 34 to 40 mm are shown in Figure 5(a). Results indicate that the two resonant modes (the dual-resonant mode at about 850 MHz

(a)

(b)
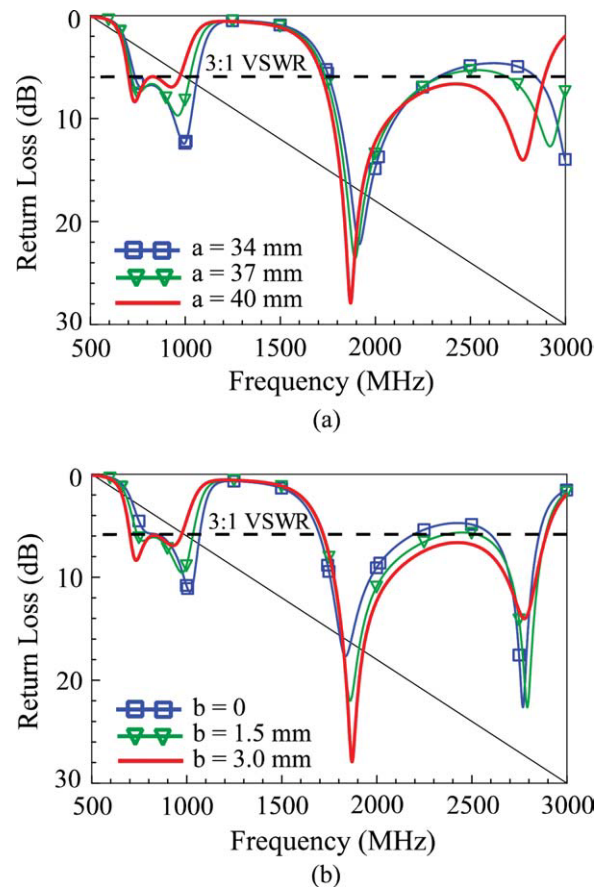
Figure 5 Simulated return loss for the proposed antenna as a function of (a) the length a and (b) the width b of the bent end-section of the strip monopole. Other dimensions are the same as given in Figure 1. [Color figure can be viewed in the online issue, which is available at wileyonlinelibrary.com]
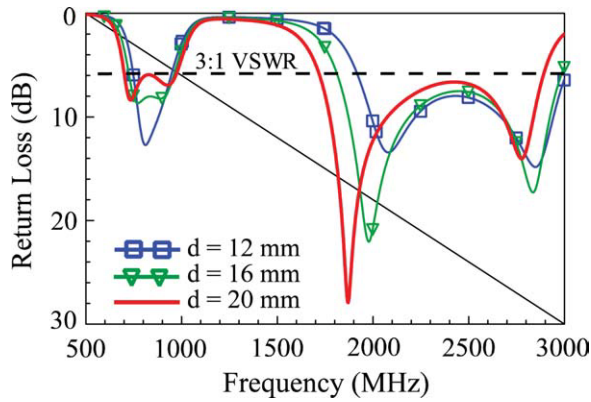
Figure 6 Simulated return loss for the proposed antenna as a function of the position d of the grounding point B. Other dimensions are the same as given in Figure 1. [Color figure can be viewed in the online issue, which is available at wileyonlinelibrary.com]

and the second mode in the antenna's upper band) mainly controlled by the strip monopole are shifted to higher frequencies with a decrease in the length a. This behavior is reasonable since the variations in the length a will cause the resonant length variations contributed by the planar strip monopole. Results for the width b varied from 0 to 3 mm are presented in Figure 5(b). The major effects are seen to be on the impedance matching of both the antenna's lower and upper bands. This behavior is also reasonable since a widened width of the strip monopole can lead to smoother surface current distributions and in turn better impedance matching to achieve enhanced impedance bandwidths [27].

Figure 6 shows the simulated return loss for the proposed antenna as a function of the position d of the grounding point B. Large effects on the first mode of the antenna's upper band are seen. This resonant mode is mainly controlled by the loop radiating feed and is seen to be shifted to either higher or lower frequencies with a variation in the position d. This indicates that the desired upper band for the proposed antenna can be controlled by adjusting the position d. At the same time, since the loop radiating feed excites the planar strip monopole, some variations on the impedance matching of the other two resonant modes controlled by the planar strip monopole are also seen.

Figure 7 shows the simulated return loss as a function of the width t of the widened section of the loop radiating feed. With
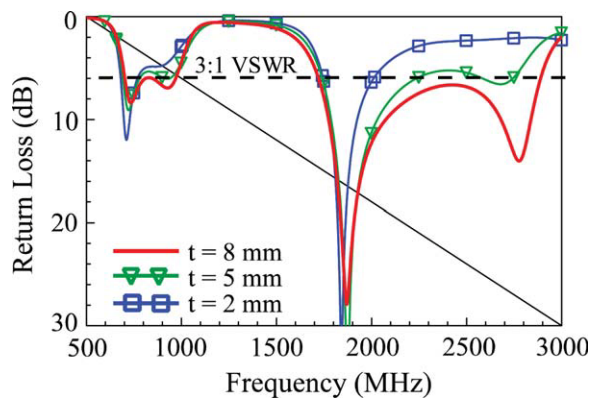
Figure 7 Simulated return loss for the proposed antenna as a function of the width t of the widened section of the loop radiating feed. Other dimensions are the same as given in Figure 1. [Color figure can be viewed in the online issue, which is available at wileyonlinelibrary.com]
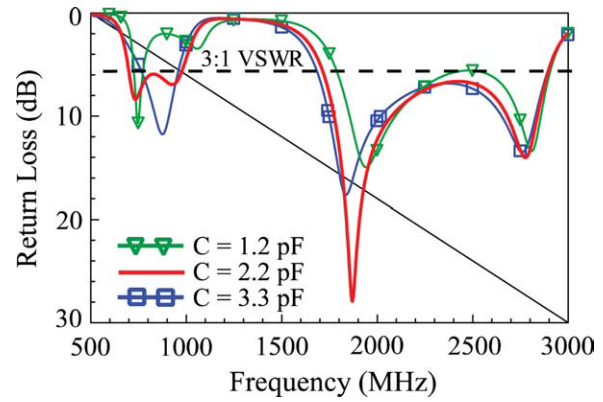
Figure 8 Simulated return loss for the proposed antenna as a function of the capacitance C of the loaded chip capacitor in the loop radiating feed. Other dimensions are the same as given in Figure 1. [Color figure can be viewed in the online issue, which is available at wileyonlinelibrary.com]

an increase in the width t, the impedance matching for all the three excited resonant modes is improved, and the bandwidths of the antenna's lower and upper bands are enhanced. Figure 8 shows the simulated return loss as a function of the capacitance C of the loaded chip capacitor in the loop radiating feed. Results for the capacitance C varied from 1.2 to 3.3 pF are presented. The major effects are seen on the dual-resonance excitation of the resonant mode in the lower band. With proper chip capacitor ($C = 2.2$ pF) loaded, good dual-resonance excitation to widen the antenna's lower-band bandwidth is obtained.

To analyze the radiation characteristics, the proposed antenna is mounted at the bottom edge of the mobile phone, and the measured three-dimensional (3D) total-power radiation patterns are plotted in Figure 9. The radiation patterns seen in four different directions [the front (x direction), back ($-x$ direction), top (z direction) and bottom ($-z$ direction) directions] are shown. Dipole-like radiation patterns at lower frequencies (740 and 925 MHz) are observed, while more variations in the radiation patterns are seen at higher frequencies (1795, 2045, and 2595 MHz). Large differences in the radiation patterns at lower and higher frequencies are related to the excited surface currents on the system ground plane of the mobile phone, and the radiation patterns of the proposed antenna show no special distinctions compared to those of the traditional internal WWAN mobile phone antennas [28]. The measured radiation efficiencies for the fabricated antenna are shown in Figure 10. The efficiencies are all better than 50%, about 57–75% and 66–90% respectively for lower and upper bands, which is acceptable for practical mobile phone applications.

Figure 11 shows the simulated 1-g SAR values for the proposed antenna mounted at the bottom edge of the mobile phone. The SAR simulation model provided by SEMCAD X version 14 [29] is also shown in the figure. The head and hand phantoms are included in the simulation model. The mobile phone is held by the hand phantom with a distance of 33 mm between the palm center and the system ground plane, which is reasonable as studied in [21]. The SAR values are tested using input power of 24 dBm for the frequencies in the GSM850/900 bands (859, 925 MHz) and 21 dBm in the GSM1800/1900/UMTS bands (1795, 1920, 2045 MHz) and LTE700/2300/2500 bands (740, 2350, 2595 MHz). The simulated SAR distributions at each frequency tested in the study are also shown. The open squares in the SAR distributions represent the local SAR maximum. The simulated SAR values for 1-g head and 1-g head and hand
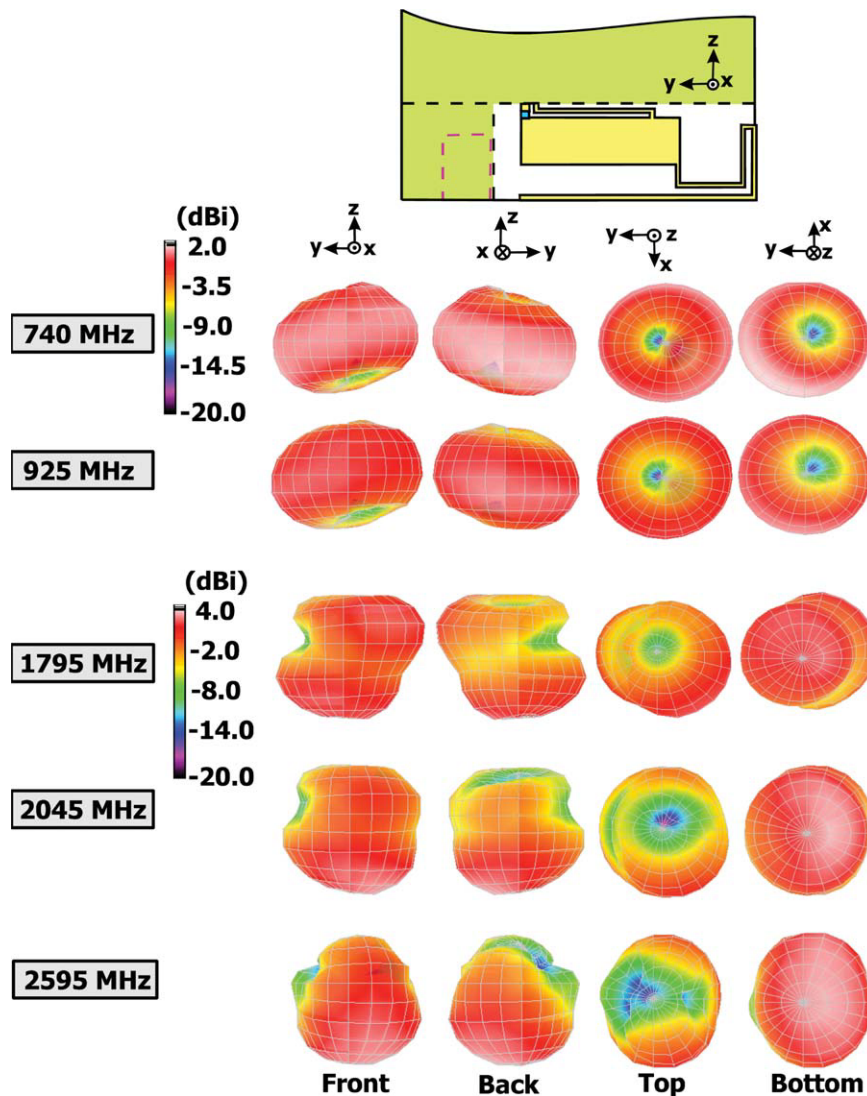
Figure 9 Measured three-dimensional (3D) total-power radiation patterns for the proposed antenna mounted at the bottom edge of the mobile phone. [Color figure can be viewed in the online issue, which is available at wileyonlinelibrary.com]
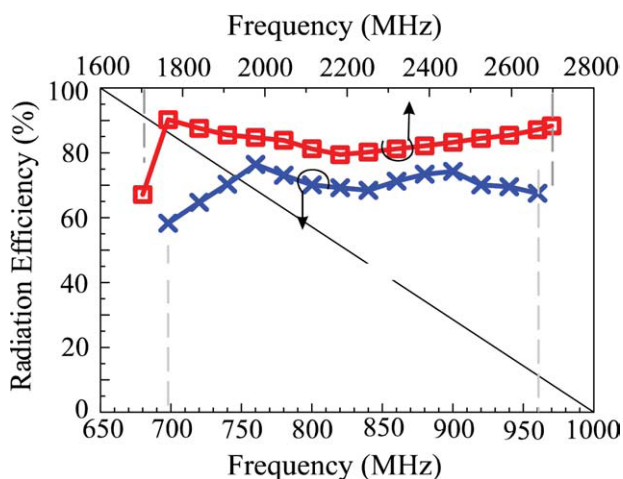
Figure 10 Measured radiation efficiency for the proposed antenna. [Color figure can be viewed in the online issue, which is available at wileyonlinelibrary.com]

tissues listed in the table in the figure are well below the limit of 1.6 W/kg for practical applications. At lower frequencies (740, 850, 925 MHz), the SAR values are about the same for the two cases of with and without the hand phantom. While at higher frequencies, especially at 2045, 2350, and 2595 MHz, the SAR values are much higher when the hand phantom is present. In these cases, the local maximum SAR value occurs at the hand phantom. This behavior is related to the smaller wavelengths at higher frequencies. The obtained SAR results make the proposed antenna very promising for practical applications.

4. CONCLUSION

An internal eight-band LTE/WWAN mobile phone antenna with a low profile and a small occupied board space has been proposed and studied. The antenna has a simple structure and is easy to fabricate at low cost. The antenna is formed by a planar strip monopole connected to a chip capacitor-loaded loop radiating feed, which not only excites the strip monopole to generate two wide resonant modes but also contributes a wide resonant mode to the proposed antenna. The three excited resonant modes form two wide operating bands, with the lower one covering the
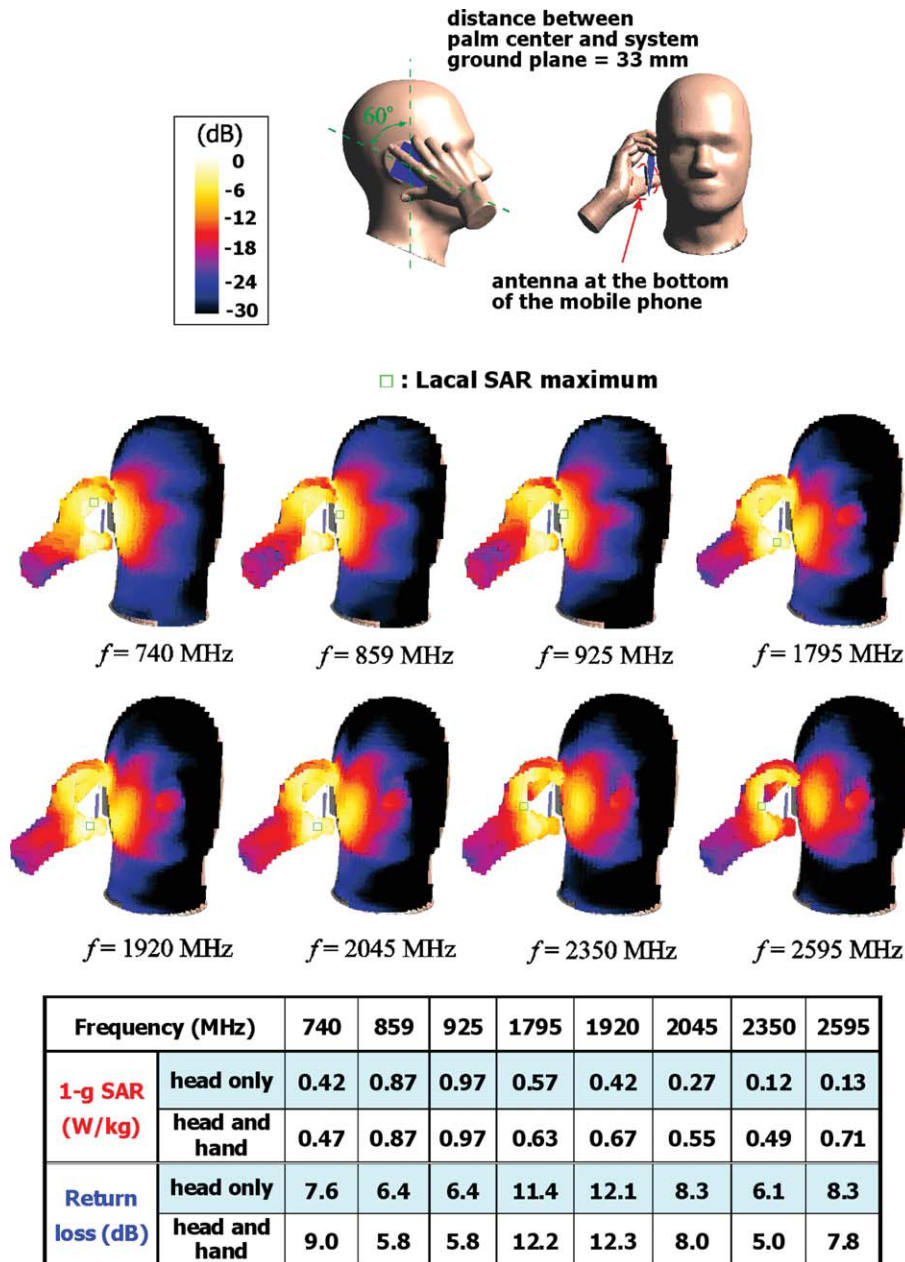
Figure 11 SAR simulation model and the simulated 1-g SAR values for the proposed antenna mounted at the bottom edge of the mobile phone. The return loss given in the table is the impedance matching level at the testing frequency. [Color figure can be viewed in the online issue, which is available at wileyonlinelibrary.com]

698–960 MHz band (LTE700/GSM850/900) and the upper one covering the 1710–2690 MHz band (GSM1800/1900/UMTS/ LTE2300/2500). The antenna can also integrate with a USB connector as the data port at the bottom edge of the mobile phone. With this structure, acceptable radiation characteristics are obtained, and the simulated 1-g SAR values over the eight operating bands are also well below the limit of 1.6 W/kg. The proposed antenna is promising for practical slim mobile phone applications.

REFERENCES

1. http://en.wikipedia.org/wiki/3GPP_Long_Term_Evolution, Wikipedia, the free encyclopedia: 3GPP Long Term Evolution.
2. T.W. Kang and K.L. Wong, Internal printed loop/monopole combo antenna for LTE/GSM/UMTS operation in the laptop computer, Microwave Opt Technol Lett 52 (2010), 1673–1678.
3. C.T. Lee and K.L. Wong, Planar monopole with a coupling feed and an inductive shorting strip for LTE/GSM/UMTS operation in the mobile phone, IEEE Trans Antennas Propagat 58 (2010), 2479–2483.
4. K.L. Wong, M.F. Tu, C.Y. Wu, and W.Y. Li, Small-size coupled-fed printed PIFA for internal eight-band LTE/GSM/UMTS mobile phone antenna, Microwave Opt Technol Lett 52 (2010), 2123–2128.
5. S.C. Chen and K.L. Wong, Bandwidth enhancement of coupled-fed on-board printed PIFA using bypass radiating strip for eight-band LTE/GSM/UMTS slim mobile phone, Microwave Opt Technol Lett 52 (2010), 2059–2065.
6. K.L. Wong, W.Y. Chen, C.Y. Wu, and W.Y. Li, Small-size internal eight-band LTE/WWAN mobile phone antenna with internal distributed LC matching circuit, Microwave Opt Technol Lett 52 (2010), 2244–2250.

7. M.F. Abedin and M. Ali, Modifying the ground plane and its effect on planar inverted-F antennas (PIFAs) for mobile phone handsets, IEEE Antennas Wireless Propag Lett 2 (2003), 226–229.

8. R. Hossa, A. Byndas, and M.E. Bialkowski, Improvement of compact terminal antenna performance by incorporating open-end slots in ground plane, IEEE Microwave Wireless Compon Lett 14 (2004), 283–285.

9. K.L. Wong, Y.C. Lin, and T.C. Tseng, Thin internal GSM/DCS patch antenna for a portable mobile terminal, IEEE Trans Antennas Propag 54 (2006), 238–242.

10. K.L. Wong, Y.C. Lin, and B. Chen, Internal patch antenna with a thin air-layer substrate for GSM/DCS operation in a PDA phone, IEEE Trans Antennas Propag 55 (2007), 1165–1172.

11. R.A. Bhatti, Y.T. Im, J.H. Choi, T.D. Manh, and S.O. Park, Ultra-thin planar inverted-F antenna for multistandard handsets, Microwave Opt Technol Lett 50 (2008), 2894–2897.

12. H. Rhyu, J. Byun, F.J. Harakiewicz, M.J. Park, K. Jung, D. Kim, N. Kim, T. Kim, and B. Lee, Multi-band hybrid antenna for ultra-thin mobile phone applications, Electron Lett 45 (2009), 773–334.

13. C.L. Tang and S.C. Lai, Multi-function IC antenna design and fabrication, In: Proceedings of the Asia-Pacific Microwave Conference, Singapore, 2009, Session TU4A, Paper no. 1741.

14. http://en.wikipedia.org/wiki/Universal_Serial_Bus, Wikipedia, the free encyclopedia: Universal Serial Bus (USB).

15. K.L. Wong, S.L. Chien, C.M. Su, and F.S. Chang, An internal planar mobile phone antenna with a vertical ground plane, Microwave Opt Technol Lett 47 (2005), 597–599.

16. C.M. Su, K.L. Wong, C.L. Tang, and S.H. Yeh, EMC internal patch antenna for UMTS operation in a mobile device, IEEE Trans Antennas Propagat 53 (2005), 3836–3839.

17. C.H. Wu and K.L. Wong, Internal shorted planar monopole antenna embedded with a resonant spiral slot for penta-band mobile phone application, Microwave Opt Technol Lett 50 (2008), 529–536.

18. Y.W. Chi and K.L. Wong, Half-wavelength loop strip fed by a printed monopole for penta-band mobile phone antenna, Microwave Opt Technol Lett 50 (2008), 2549–2554.

19. M.R. Hsu and K.L. Wong, WWAN ceramic chip antenna for mobile phone application, Microwave Opt Technol Lett 51 (2009), 103–110.

20. American National Standards Institute (ANSI), Safety levels with respect to human exposure to radio-frequency electromagnetic field, 3 kHz to 300 GHz, ANSI/IEEE standard C95.1, April 1999.

21. C.H. Li, E. Ofli, N. Chavannes, and N. Kuster, Effects of hand phantom on mobile phone antenna performance, IEEE Trans Antennas Propagat 57 (2009), 2763–2770.

22. K.L. Wong and C.H. Huang, Bandwidth-enhanced internal PIFA with a coupling feed for quad-band operation in the mobile phone, Microwave Opt Technol Lett 50 (2008), 683–687.

23. C.H. Chang and K.L. Wong, Internal coupled-fed shorted monopole antenna for GSM850/900/1800/1900/UMTS operation in the laptop computer, IEEE Trans Antennas Propag 56 (2008), 3600–3604.

24. K.L. Wong and S.J. Liao, Uniplanar coupled-fed printed PIFA for WWAN operation in the laptop computer, Microwave Opt Technol Lett 51 (2009), 549–554.

25. C.T. Lee and K.L. Wong, Uniplanar coupled-fed printed PIFA for WWAN/WLAN operation in the mobile phone, Microwave Opt Technol Lett 51 (2009), 1250–1257.

26. Ansoft Corporation HFSS. Available at http://www.ansoft.com/products/hf/hfss/.

27. Y.L. Kuo and K.L. Wong, Printed double-T monopole antenna for 2.4/5.2 GHz dual-band WLAN operations, IEEE Trans Antennas Propagat 51 (2003), 2187–2192.

28. K.L. Wong, Planar antennas for wireless communications, Wiley, New York, 2003.

29. http://www.semcad.com, SEMCAD, Schmid & Partner Engineering AG (SPEAG).

NOISE SENSOR BASED ON A FIBER BRAGG GRATING AND A PIEZO-ELECTRIC TRANSDUCER

Chin-Hsing Cheng, Lung-Hui Lai, and Wen-Fung Liu

Department of Electrical Engineering, Feng Chia University No.100, Wen Hwa Rd., Taichung 407, Taiwan, Republic of China; Corresponding author: chcheng@fcu.edu.tw

ABSTRACT: *This article demonstrates an optical fiber sensor using fiber Bragg grating (FBG) and a Piezo-electrical transducer (PZT) to measure noise. Mounting an FBG on a PZT bar, a dynamic strain simulator was constructed. The voltage produced by noise level applied on PZT was converted to the dynamic variation of FBG Bragg wavelength. The experiments showed that the sensitivity of center-wavelength variations is 0.0129 nm/dB for noise measurement between 85.3 and 105.2 dB.* © 2011 Wiley Periodicals, Inc. Microwave Opt Technol Lett 53:958–961, 2011; View this article online at wileyonlinelibrary.com. DOI 10.1002/mop.25844

1. INTRODUCTION

In environmental and industrial acoustics, a common issue is the identification of the contribution of specific sources to global levels. Such issues can occur inside a factory when one wants to identify noisy machines to control their emissions or in environmental monitoring when the goal is the evaluation of the acoustic impact of a source on already noisy neighborhoods [1]. Several noise determination methods have been suggested based on the sound pressure level obtained from a receiver [2–4].

Optical fiber gratings are currently used as sensors for a number of physical magnitudes such as temperature, strain and pressure [5, 6]. Through the years, a number of different optical systems for current measurement applications have been presented. The previous works are focused on the applications of fiber grating electric power and current sensors [7, 8]. The main field of interest has been devices intended to replace conventional current meters by utilizing the nonconductive nature of the optical components. As optical measurement systems tend to be much smaller and lighter than their conventional equivalents, this technique also makes it possible to produce portable equipment.

In this article, we demonstrate a new approach to noise measurement [9, 10]. The relationship between the electrostrictive characteristic of Piezo-electrical transducer (PZT) and the driving voltage is linear. When applying voltage to the PZT, the material will distort to a certain displacement, and the Bragg wavelength of the fiber Bragg grating (FBG) plastered on the surface of the PZT will also change. The voltage measurement produced by noise level will be achieved by measuring the changing value of the wavelength [11].

2. PRINCIPLES

Sound is measured by the amplitude of the pressure fluctuations on the human ear. For convenience, it is expressed as a ratio between the measured pressure and an agreed reference level of $p_{re} = 20 \times 10^{-6}$ Pa as follows:

$$L_P = 10 \, \log_{10} \left(\frac{p^2}{p_{re}^2} \right) \tag{1}$$